[3] a) M. J. Plunkett, J. A. Ellman in *Combinatorial Chemistry McGraw-Hill Yearbook of Science & Technology* (Ed.: S. P. Parker), McGraw-Hill, New York, **1997**, pp. 95 – 99; b) D. Obrecht, J. M. Villalgordo, *Solid-Supported Combinatorial and Parallel Synthesis of Small-Molecular-Weight Compounds Libraries*, *Vol. 17*, Pergamon Elsevier, Oxford, **1998**; c) T. R. Boussie, C. Coutard, H. Turner, V. Murphy, T. S. Powers, *Angew. Chem.* **1998**, *110*, 3472 – 3475; *Angew. Chem. Int. Ed.* **1998**, *37*, 3272 – 3275; d) A. Holzwarth, H. W. Schmidt, W. F. Maier, *Angew. Chem.* **1998**, *110*, 2788 – 2792; *Angew. Chem. Int. Ed.* **1998**, *37*, 2644 – 2650; e) B. Jandeleit, D. J. Schaefer, T. S. Powers, H. W. Turner, W. H. Weinberg, *Angew. Chem.* **1999**, *111*, 2648 – 2689; *Angew. Chem. Int. Ed.* **1999**, *38*, 2494 – 2532; f) A. Berkessel, D. A. Herault, *Angew. Chem.* **1999**, *111*, 99 – 102; *Angew. Chem. Int. Ed.* **1999**, *38*, 102 – 105.

[4] a) S. Itsuno, Y. Sakurai, K. Ito, T. Maruyama, S. Nakahama, J. M. J. Fréchet, *J. Org. Chem.* **1990**, *55*, 304 – 310; b) K. Kamahori, S. Tada, K. Ito, S. Itsuno, *Tetrahedron: Asymmetry* **1995**, *6*, 2547 – 2555; c) P. Salvadori, D. Pini, A. Petri, *Synlett* **1999**, 1181 – 1190; d) D. A. Annis, E. N. Jacobsen, *J. Am. Chem. Soc.* **1999**, *121*, 4147 – 4154.

[5] a) J. M. Fraile, J. A. Mayoral, A. J. Royo, R. V. Salvador, B. Altava, S. V. Luis, M. I. Burguete, *Tetrahedron* **1996**, *52*, 9853 – 9862; b) B. Altava, M. I. Burguete, E. García-Verdugo, S. V. Luis, R. V. Salvador, M. J. Vicent, *Tetrahedron* **1999**, *55*, 12 897 – 12 906; c) B. Altava, M. I. Burguete, E. García-Verdugo, S. V. Luis, O. Pozo, R. V. Salvador, *Eur. J. Org. Chem.* **1999**, 2263 – 2267; for related studies on polysiloxanes, see d) M. Reggelin, *Nachr. Chem. Tech. Lab.* **1997**, *45*, 1196 – 1201, and references therein.

[6] a) D. Seebach, B. Weidmann, L. Widler in *Modern Synthetic Methods*, *Vol. 3* (Ed.: R. Scheffold), Wiley, New York, **1983**, pp. 217 – 353; b) K. Narasaka, M. Inoue, T. Yamada, J. Sugimori, N. Iwasawa, M. Nakashima, *J. Am. Chem. Soc.* **1989**, *111*, 5340 – 5345; c) K. Narasaka, *Synthesis* **1991**, 1 – 11; d) D. Seebach, R. Dahinden, R. E. Marti, A. K. Beck, D. A. Plattner, F. N. M. Kühnle, *J. Org. Chem.* **1995**, *60*, 1788 – 1799; e) H. Sellner, D. Seebach, *Angew. Chem.* **1999**, *111*, 2039 – 2041; *Angew. Chem. Int. Ed.* **1999**, *38*, 1918 – 1920.

[7] a) D. Seebach, R. E. Marti, T. Hintermann, *Helv. Chim. Acta* **1996**, *79*, 1710 – 1740, and references therein; b) J. M. Fraile, J. A. Mayoral, A. J. Royo, B. Altava, M. I. Burguete, B. Escuder, S. V. Luis, R. V. Salvador, *J. Org. Chem.* **1997**, *62*, 3126 – 3134; c) J. Irurre, A. Fernandez-Serrat, M. Altayo, M. Riera, *Enantiomer* **1998**, *3*, 103 – 120; d) B. P. Santora, P. S. White, M. R. Gagné, *Organometallics* **1999**, *18*, 2557 – 2560.

[8] a) B. Altava, M. I. Burguete, J. M. Fraile, J. I. García, S. V. Luis, J. A. Mayoral, A. J. Royo, M. J. Vicent, *Tetrahedron: Asymmetry* **1997**, *8*, 2561 – 2570; for different mechanistic models, see b) Y. N. Ito, X. Ariza, A. K. Beck, A. Bohác, C. Ganter, R. E. Gawley, F. N. M. Kühnle, J. Tuleja, Y. M. Wang, D. Seebach, *Helv. Chim. Acta* **1994**, *77*, 2071 – 2110; c) K. V. Gothelf, K. A. Jørgensen, *J. Org. Chem.* **1995**, *60*, 6847 – 6851; d) C. Haase, C. R. Sarko, M. DiMare, *J. Org. Chem.* **1995**, *60*, 1777 – 1787; e) K. V. Gothelf, R. G. Hazell, K. A. Jørgensen, *J. Am. Chem Soc.* **1995**, *117*, 4435 – 4436.

[9] a) F. Svec, J. M. J. Fréchet, *Chem. Mater.* **1995**, *7*, 707 – 715; b) F. Svec, J. M. J. Fréchet, *Science* **1996**, *273*, 205 – 211, and references therein; c) S. Xie, F. Svec, J. M. J. Fréchet, *Chem. Mater.* **1998**, *10*, 4072 – 4078; d) F. Svec, J. M. J. Fréchet, *Ind. Eng. Chem. Res.* **1999**, *38*, 34 – 48.

[10] All TADDOL derivatives were prepared starting from dimethyl L-tartrate. This was the only tartrate stereoisomer present in our laboratory during this work so as to avoid accidental contamination or preparation of the wrong TADDOL isomer. When reversal of topicity was observed, the optical rotation of the starting material was checked and gave the expected value for the methyl ester of L-tartaric acid ($[\alpha]_D^{22} = 21$ ($c = 0.20$, H_2O)). Duplication of the whole experiment using this tested starting material gave the same results.

[11] a) G. Wulff, R. Kemmerer, B. Vogt, *J. Am. Chem. Soc.* **1987**, *109*, 7449 – 7457; b) G. Wulff, *Angew. Chem.* **1995**, *107*, 1958 – 1979; *Angew. Chem. Int. Ed. Engl.* **1995**, *34*, 1812 – 1832; c) G. Wulff, S. Gladow, S. Krieger, *Macromolecules* **1995**, *28*, 7434 – 7440; d) C. Alexander, C. R. Smith, M. J. Whitcombe, E. N. Vulfson, *J. Am. Chem. Soc.* **1999**, *121*, 6640 – 6651.

Polymeric Layers Catenated by Ribbons of Rings in a Three-Dimensional Self-Assembled Architecture: A Nanoporous Network with Spongelike Behavior

Lucia Carlucci, Gianfranco Ciani,* Massimo Moret, Davide M. Proserpio, and Silvia Rizzato

The current interest in the crystal engineering of polymeric coordination networks[1] stems from their potential applications as zeolite-like materials[2] for molecular selection, ion exchange, and catalysis, as well as in the intriguing variety of architectures and topologies. Particularly attractive are the novel types of supramolecular intertwinings observed in these species, that still need a rational classification. According to Batten and Robson[3] an "interpenetrating framework" is comprised of motifs that are infinite and inextricably entangled, that is, they cannot be separated without breaking links. On this basis, we must exclude some interesting polymeric entanglements recently described, including polymeric catenanes,[4] infinite double helices,[5] two-dimensional clothlike warp-and-weft sheets,[6] and other noteworthy supramolecular architectures.[7] For "true" interpenetrating networks, however, different classes can be envisaged. The dominant type ("class A") is represented by 2D or 3D species that are comprised of a limited number of individual frames of equal topology that interpenetrate into an array with the same original dimensionality as in, for example, *n*-fold parallel interpenetrating hexagonal layers ($n \leq 6$) or diamondoid nets ($n \leq 9$).[3] Other types of interpenetration have been observed in coordination polymers that are reminiscent of molecular catenanes and rotaxanes. Some examples of polymeric catenated species are illustrated in Figure 1. In contrast to the class A interpenetrated nets, these examples all show the following features: 1) the constituent motifs have a lower dimensionality than that of the resulting architectures; 2) each individual motif is intertwined only with the surrounding ones and not with all the others, as "a ring in a chain"; and 3) the concept of "*n*-foldicity" cannot be used in the same sense as for class A.[13] We report here on a new member of this class of catenated motifs, **1**, obtained from the self-assembly of copper(II) sulfate and 1,3-bis(4-pyridyl)propane (bpp).

$[Cu_5(bpp)_8(SO_4)_4(EtOH)(H_2O)_5](SO_4) \cdot EtOH \cdot 25.5\ H_2O$ **1**

[*] Prof. G. Ciani, Prof. M. Moret, Dr. D. M. Proserpio, Dr. S. Rizzato
Dipartimento di Chimica Strutturale e Stereochimica Inorganica
and Centro CNR
Universitá di Milano
Via G. Venezian 21, 20133 Milano (Italy)
Fax: +(390) 2-70635288
E-mail: davide@csmtbo.mi.cnr.it

Dr. L. Carlucci
Dipartimento di Biologia Strutturale e Funzionale
Universita' dell'Insubria
Via J. H. Dunant 3, 21100 Varese (Italy)

Supporting information for this article is available on the WWW under http://www.wiley-vch.de/home/angewandte/ or from the author.

  0044-8249/00/11208-1566 $ 17.50+.50/0

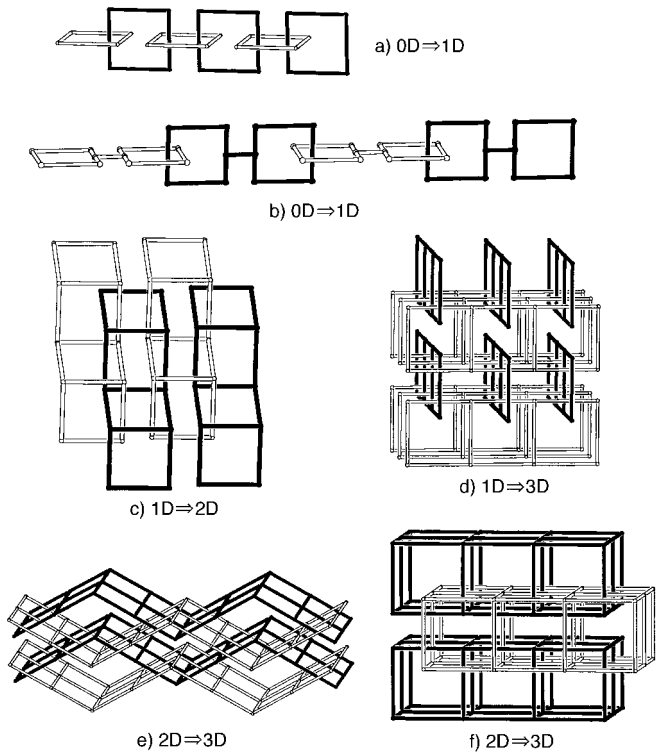

Figure 1. Schematic examples of polymeric catenated structures. Motifs b)–f) are simplified versions of entanglements found in real species: b) a poly[2]catenane;[4, 8] c) parallel interpenetration of ladders;[9] d) inclined interpenetration of ladders;[10] e) catenation of simple undulating layers;[11] f) catenation of multiple layers.[12] No real example of an infinite polycatenane of type (a) has yet been reported.

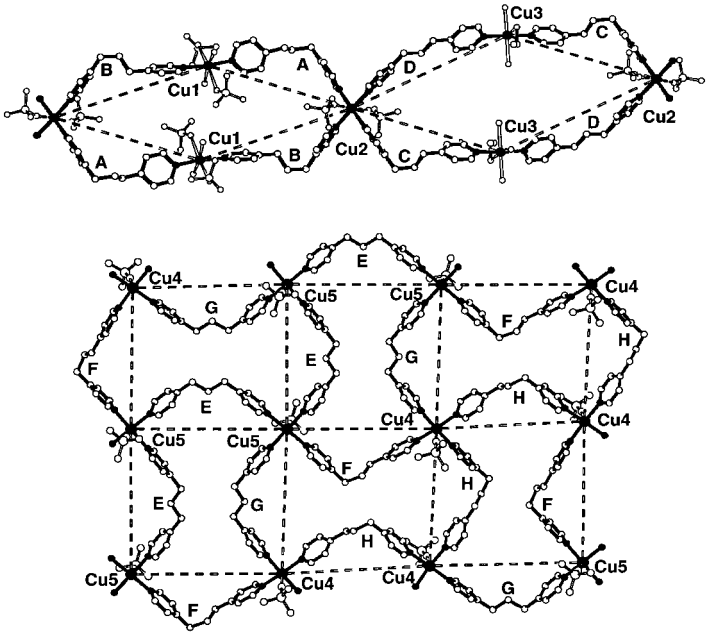

Figure 2. The two polymeric motifs present in **1** are a ribbon of rings (top) and a (4,4) layer (bottom). The eight independent bpp ligands are labelled A–H and show conformations *TG*, *TG*, *TG*, *TT*, *TT*, *TG*, *TT*, and *TG*, respectively (T = trans, G = gauche). Bond distances [Å] involving the copper atoms are: in the rings: Cu2–N (four bonds) 2.050(5)–2.068(4); $Cu2–O_{sulfate}$ (two bonds) 2.418(4), 2.523(4); Cu1–N (two bonds) 2.020(5), 2.027(5); $Cu1–O_{sulfate}$ (two bonds) 2.435(4), 2.508(4); $Cu1–O_{water}$ (two bonds) 2.001(4), 2.034(4); Cu3–N (two bonds) 2.015(5), 2.032(5); $Cu3–O_{water}$ (three bonds) 2.167(6)–2.333(5); $Cu3–O_{ethanol}$ 2.137(7); in the layer: Cu4–N, Cu5–N (four bonds each) 2.034(5)–2.066(5); $Cu4–O_{sulfate}$ 2.385(4); $Cu5–O_{sulfate}$ 2.305(4).

This species presents a remarkable and unprecedented three-dimensional architecture sustained by the polycatenation of two different types of coordination polymers, that is, one-dimensional ribbons of rings and two-dimensional (4,4) layers. It shows, moreover, an interesting nanoporous behavior due to the presence of large cavities full of guest solvent molecules. These solvent species can be completely removed by thermal treatment and regained in a reversible process, to imply some degree of flexibility in the network.

Compound **1** is obtained in high yields as beautiful blue crystals by the slow diffusion of bpp as an ethanol solution into copper(II) sulfate as an aqueous solution, with metal: ligand molar ratios ranging from 1:1 to 1:4. Similar crystalline species are also obtained using other solvents for the ligand (acetone, ethyl acetate, tetrahydrofuran), as shown by X-ray diffraction measurements on the powders. Although crystals start to lose solvated water and ethanol molecules when removed from their mother liquor, they reach an equilibrium at room temperature and display the same X-ray powder diffraction (XRPD) pattern even after two months in the air. Crystals taken from the solution for the XRPD experiments (at 223 K) were manipulated in an ice bath.[14]

The crystal structure of **1** shows the presence of two different and crystallographically independent polymeric motifs packed together (Figure 2). One motif, the ribbons of rings, consists of 48-membered cycles, in which each ring includes four copper atoms and four bpp ligands. The ribbons undulate slightly, with the metal atoms disposed at the vertices of rhombuses (Cu···Cu 11.80–13.53 Å). All these polymers run parallel to the $[10\bar{1}]$ direction with a 47.24 Å period corresponding to two successive rings. Adjacent ribbons show a relative displacement of ¼ of this period. The copper atoms shared by adjacent rings (Cu2) are connected to four bpp ligands, whereas the lateral Cu1 and Cu3 atoms are connected to two such ligands. The octahedral coordination geometries of these metals are completed by sulfate anions and solvent molecules.

The other polymeric motif of **1** is a two-dimensional tessellated sheet of (4,4) topology (Figure 2 bottom) which contains two types of copper atoms, Cu4 and Cu5, and four types of bpp ligands. Within these layers, the copper atoms are located at the nodes of a square grid with edges 11.93–12.49 Å long. Both copper atoms are connected to four equatorial pyridyl rings and are bonded to an oxygen atom of a sulfate group in an axial direction, to form a square-pyramidal coordination. These sulfate anions are the same involved in axial interactions with the Cu2 atoms of the ribbons and represent the only bridge between the two types of polymers. The layers stack in the $[10\bar{1}]$ direction with an *ABCD* sequence.

The most interesting structural feature of **1**, however, is that the ribbons and the layers are entangled (Figure 3) in a unique three-dimensional array. Each ring of the ribbons locks two adjacent layers and each "square" mesh of the layers is

  0044-8249/00/11208-1567 $ 17.50+.50/0

Figure 3. The entanglement of one ribbon with two adjacent layers. Only the metal atoms and the bpp ligands (without hydrogen atoms) are shown.

catenated by two rings belonging to different ribbons. The overall architecture is schematically represented in Figure 4. Few examples of entangled polymeric species with a differing nature, with either identical or different topologies,[3] are presently known, but this is, to our knowledge, the first example of intertwining involving two polymeric motifs of different (1D and 2D) dimensionality.

The coordination network of **1** contains large voids in the interlayer regions (interlayer separation approximately 11.8 Å), which are filled by solvated molecules of water and ethanol (102 and 4 solvent molecules per unit cell, respectively). An analysis of these regions, by neglecting all the solvent molecules but those coordinated to the copper atoms, shows that there are two type of large, isolated chambers of volumes around 790 and 670 $Å^3$ and smaller holes of 140 $Å^3$ (two, two, and four per unit cell, respectively; Figure 5).[15] The total void space in a unit cell corresponds to 3626 $Å^3$, equivalently, 25.8 % of the cell volume. The uncoordinated solvent molecules display a variety of environments and form an intricate, extended net of hydrogen bonds. According to the structural data they can be roughly assigned as: a) tightly bonded molecules, anchored to the network by two or more hydrogen-bond bridges involving the coordinated sulfate or water molecules; b) molecules with "intermediate" bonding, with only one such hydrogen bond described under (a); and c) loosely bonded molecules showing only contacts with other solvated molecules. Group a) includes the free ethanol and about 27 % of the solvated water, group b) accounts for about 24 % of the solvated water, while the majority (49 %) of the water falls into group c). Such distribution is reflected in the nanoporous behavior of this material. When the crystals are removed from the solution they begin to weep solvent. Thermogravimetric analysis (TGA) at room temperature under a N_2 flux shows that an equilibrium situation is achieved after about 100 min, with a 13.5 % mass loss (approximately corresponding to the loss of the free ethanol and the solvated H_2O of groups b) and c)). Equilibration in the air at room temperature occurs after an initial mass loss, estimated of 2–4 % but this value is very sensitive to temperature and humidity. At this point most of the crystals under the microscope appear almost unchanged in morphology and color but they do not remain monocrystalline. These polycrystalline samples exhibit XRPD spectra quite similar to that simulated from the single crystal structure.[16] Desolvation can be completed by thermal activation and TGA in the range 40–180 °C shows an almost continuous weight loss. On heating to about 120 °C, all of the guest molecules are eliminated,[17] while the coordinated solvents are lost in the range 120–180 °C (mass loss 3–4 %); the decomposition of the network starts above 200 °C. Monitoring the samples heated to different temperatures (50, 95, 120, 150 °C) reveals a progressive loss of crystallinity—with a significant change of the pattern above 90 °C—resulting in an almost completely amorphous phase. However, these samples left in the presence of water vapors at room temperature for some hours regain solvent (specifically, solvent groups a), b), and about half of c) to correspond to the equilibrium situation described above) and, unexpectedly, crystallinity, showing XRPD patterns identical to the original one. The cycle of desolvation–solvation can be repeated many times as controlled by TGA and monitored by XRPD.[18] Only after elimination of the coordinated solvent molecules does the array become unstable.

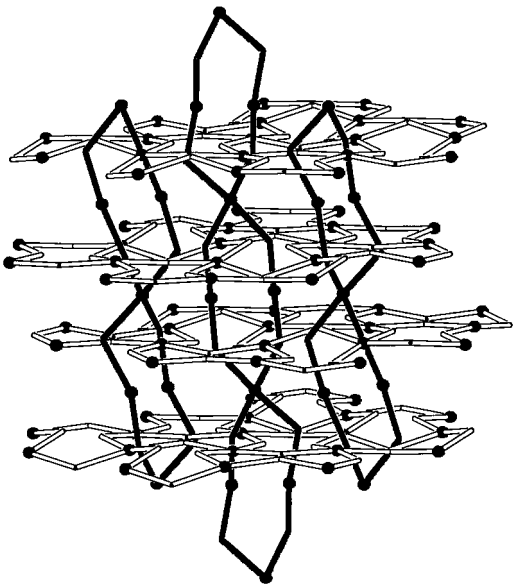

Figure 4. Schematic view of the overall entanglement of **1**. The representation of the bpp ligands is simplified by showing only the central methylene atoms.

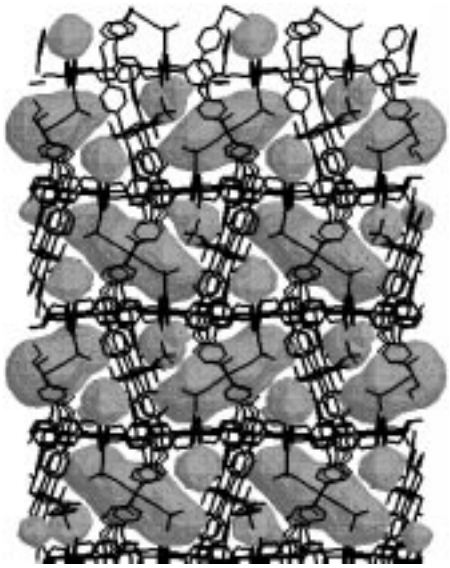

Figure 5. View down the [101] axis of the three-dimensional array of **1** showing the distribution of the empty cavities. The cavities are represented by their limiting surfaces. The layers run horizontally and the ribbons vertically.

  0044-8249/00/11208-1568 $ 17.50+.50/0

The desolvation of **1** is accompanied by a (reversible) loss of order, probably due to the local structural modifications following the spongelike shrinking of the chambers.[19] This is possible due to the variable ligand conformations and to the flexibility of the catenated architecture. For more information on this behavior, we examined **1** by atomic force microscopy (AFM). A sample of **1** was left in the air for several hours (at approximately 25 °C and 50% relative humidity) to observe the initial stages of desolvation on the [10$\bar{1}$] surface. About 45 min after removal of **1** from its mother liquor, cracks start to appear roughly running orthogonal to [010]. As time elapses, these existing cracks enlarge to 1.5 μm wide (Figure 6a) and accompany the random formation of new ones (Figure 6b). The net of cracks produces a mosaiclike surface with a significant misalignment of the crystal blocks. Cracks parallel to [010] also develop but they shift to the (apparently favored) perpendicular direction. After about 7 h, the cracks are about 4 μm wide (Figure 6c). The shrinking of the crystal is also demonstated by the height of the macrosteps on the crystal surface decreasing by 10–15% during the first 8 h of the experiment. Interestingly, on leaving the partially desolvated crystal overnight in a sealed AFM fluid cell connected to a water vapor reservoir, spontaneous water uptake from the air produces a partial healing of the cracks (Figure 6d). An attempt to follow the rehydration by AFM of a crystal heated up to 120 °C was hampered by rapid water uptake causing large surface movement that was beyond the imaging capability of the AFM. Though the evolution of cracks in relation to the network structure remains difficult to explain, it is clearly a consequence of mechanical strain following the depletion of the cavities.

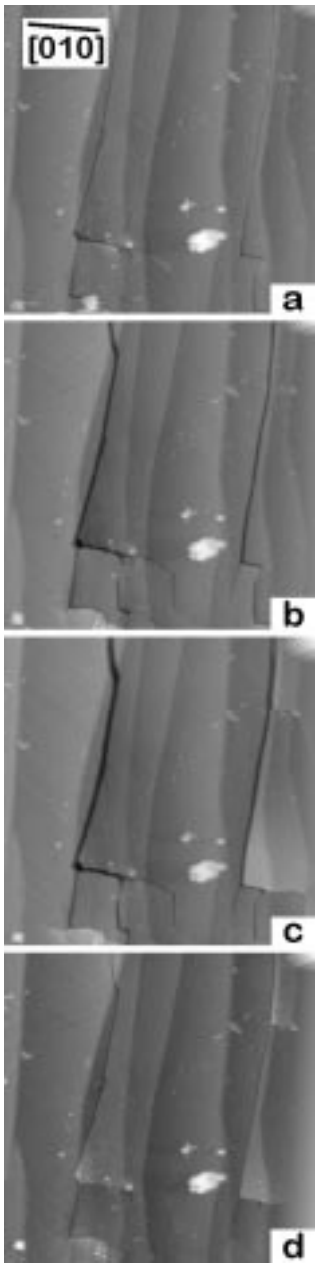

Figure 6. AFM snapshots of the desolvation sequence. Scan area $100 \times 100\ \mu m^2$. Several macrosteps 100–300 nm high running perpendicular to [010] are evident. a) 110 min: the first cracks 1.5 μm wide orthogonal to [010] appear. b) 170 min: cracks continue to enlarge and small, misaligned blocks appear. c) 460 min: main cracks are now 4 μm wide and intercalated with smaller blocks. d) 26 h: a partial healing of the crystalline surface by exposure to water vapor for a few hours is evident.

In conclusion, the fascinating three-dimensional catenated structure of **1**, with more than ¼ of its volume available for guest molecules, contains a mobility not present in the common rigid zeolite-like networks.[20] It can be considered prototypical of a new family of "nonrigid", nanoporous, spongelike coordination frames assembled with long, flexible, polydentate ligands.

Experimental Section

Synthesis of **1**: A solution of 1,3-bis(4-pyridyl)propane (bpp) (0.097 g, 0.488 mmol) in EtOH (8 mL) was added to a stirred solution of $CuSO_4 \cdot 5H_2O$ (0.061 g, 0.244 mmol) in water (8 mL) at room temperature. A blue precipitate formed immediately. The reaction mixture was stirred for 1 h. The precipitate was filtered and dried in the air (yield > 90%). The purity of these powdered samples was confirmed by XRPD. Compound **1** is sparingly soluble in polar organic solvents. Variable elemental analyses were obtained due to the loss of solvent molecules to the air (3–4%). For example, elemental analysis for $C_{108}H_{185}Cu_5N_{16}O_{52.5}S_5$: calcd: C 42.87, H 6.16, N 7.41; found: C 42.96, H 6.11, N 7.67. Single crystals suitable for structural analysis were obtained by slow diffusion of an ethanolic solution of bpp into an aqueous solution of the copper salt at a molar ratio 2:1. The presence of ethanol in **1** has been confirmed by ^{1}H NMR on solutions obtained by suspending some crystals in [D$_6$]acetone. Thermal analyses were performed on Perkin-Elmer DSC7 and TGA7 instruments at a heating rate of 10 °C min^{-1} under a nitrogen flux. X-ray powder diffraction spectra were collected on a Rigaku D/Max horizontal-scan diffractometer. A Digital Instruments "Nanoscope III" AFM, equipped with a J-type piezo scanner, operated in contact mode in the air or using a standard fluid cell for water uptake experiments. Silicon nitride cantilevers with integrated tips and nominal spring constants of 0.06–0.12 N m^{-1} were used. The tip–sample contact force was reduced to the order of a few nN to minimize artifacts and surface erosion phenomena. The scan frequency was 3–4 Hz. All images shown represent unfiltered height data.

Received: November 19, 1999 [Z14298]

[1] a) B. F. Hoskins, R. Robson, *J. Am. Chem. Soc.* **1990**, *112*, 1546; b) R. Robson, B. F. Abrahams, S. R. Batten, R. W. Gable, B. F. Hoskins, J. Liu, *Supramolecular Architecture*, Chap. 19, American Chemical Society, Washington **1992**; c) O. M. Yaghi, H. Li, C. Davis, D. Richardson, T. L. Groy, *Acc. Chem. Res.* **1998**, *31*, 474; d) M. Munakata, L. P. Wu, T. Kuroda-Sowa, *Adv. Inorg. Chem.* **1999**, *46*, 173; e) P. J. Hagrman, D. Hagrman, J. Zubieta, *Angew. Chem.* **1999**, *111*, 2798; *Angew. Chem. Int. Ed.* **1999**, *38*, 2638.

[2] For examples, see: a) C. Janiak, *Angew. Chem.* **1997**, *109*, 1499; *Angew. Chem. Int. Ed. Engl.* **1997**, *36*, 1431; b) C. J. Kepert, M. J. Rosseinsky, *Chem. Commun.* **1998**, 31; c) D. M. L. Goodgame, D. A. Grachvogel, D. J. Williams, *Angew. Chem.* **1999**, *111*, 217; *Angew. Chem. Int. Ed.* **1999**, *38*, 153.

[3] S. R. Batten, R. Robson, *Angew. Chem.* **1998**, *110*, 1558; *Angew. Chem. Int. Ed.* **1998** *37*, 1460.

[4] C. Hamers, O. Kocian, F. M. Raymo, J. F. Stoddard, *Adv. Mater.* **1998**, *10*, 1366, and references therein.

[5] a) L. Carlucci, G. Ciani, D. W. von Gudenberg, D. M. Proserpio *Inorg. Chem.* **1997**, *36*, 3812; b) O. Mamula, A. von Zelewsky, T. Bark, G. Bernardinelli, *Angew. Chem.* **1999**, *111*, 3129; *Angew. Chem. Int. Ed.* **1999**, *38*, 2945.

[6] P. M. van Calcar, M. M. Olmstead, A. L. Balch, *J. Chem. Soc. Chem. Commun.* **1995**, 1773.

[7] a) L. Carlucci, G. Ciani, D. M. Proserpio, *Chem. Commun.* **1999**, 449; b) C. V. K. Sharma, R. D. Rogers, *Chem. Commun.* **1999**, 83; c) D. Hagrman, R. P. Hammond, R. Haushalter, J. Zubieta, *Chem. Mater.* **1998**, *10*, 2091; d) M. Kondo, T. Joshitomi, K. Seki, H. Matsuzaka, S. Kitagawa, *Angew. Chem.* **1997**, *109*, 1844; *Angew. Chem. Int. Ed. Engl.*

1997, *36*, 1725; e) K. N. Power, T. L. Hennigar, M. J. Zaworotko, *New J. Chem.* **1998**, 177.

[8] J.-L. Weidmann, J.-M. Kern, J.-P. Sauvage, D. Muscat, S. Mullins, W. Köhler, C. Rosenauer, H. J. Räder, K. Martin, Y. Geerts, *Chem. Eur. J.* **1999**, *5*, 1841, and references therein.

[9] A. J. Blake, N. R. Champness, A. Khlobystow, D. A. Lenenovkii, W.-S. Li, M. Schröder, *Chem. Commun.* **1997**, 2027.

[10] a) M. Fujita, Y. J. Kwon, O. Sasaki, K. Yamaguchi, K. Ogura, *J. Am. Chem. Soc.* **1995**, *117*, 7287; b) L. Carlucci, G. Ciani, D. M. Proserpio, *J. Chem. Soc. Dalton Trans.* **1999**, 1799; c) Y.-B. Dong, R. C. Layland, M. D. Smith, N. G. Pschirer, U. H. F. Bunz, H.-C. zur Loye, *Inorg. Chem.* **1999**, *38*, 3056.

[11] M.-L. Tong, X.-M. Chen, B.-H. Ye, L.-N. Ji, *Angew. Chem.* **1999**, *111*, 2376; *Angew. Chem. Int. Ed.* **1999**, *38*, 2237.

[12] a) F.-Q. Liu, T. D. Tilley, *Inorg. Chem.* **1997**, *36*, 5090; b) L. Carlucci, G. Ciani, P. Macchi, D. M. Proserpio, S. Rizzato, *Chem. Eur. J.* **1999**, *5*, 237.

[13] These topological properties apply also to systems based on the inclined interpenetration of 2D layers (examples are given in ref. [3], sect. 3.2) and even to the remarkable polyrotaxane reported in: B. F. Hoskins, R. Robson, D. A. Slizys, *J. Am. Chem. Soc.* **1997** *119*, 2952.

[14] Crystal data for **1**: $C_{108}H_{185}Cu_5N_{16}O_{52.5}S_5$, monoclinic, space group $P2_1/c$ (no. 14), $a = 27.774(2)$, $b = 17.752(1)$, $c = 30.147(2)$ Å, $\beta = 109.22(1)^\circ$, $V = 14035(2)$ Å^3, $Z = 4$, $\rho_{calcd} = 1.432$ mg m^{-3}, $R = 0.0657$ for 15358 independent reflections [$I > 2\sigma(I)$]. The data collections were performed at 223 K on a Bruker SMART CCD area-detector diffractometer, using $Mo_{K\alpha}$ radiation ($\lambda = 0.71073$ Å) using the ω-scan method within the limits $1 < \theta < 25^\circ$. Empirical absorption corrections (SADABS) were applied. The structure was solved by direct methods (SIR97) and refined by full-matrix least-squares on F^2 (SHELX-97). Anisotropic thermal factors were assigned to all the nonhydrogen atoms except the water molecules with half occupancy. All diagrams were generated using the SCHAKAL 97. Crystallographic data (excluding structure factors) for the structure reported in this paper has been deposited with the Cambridge Crystallographic Data Centre as supplementary publication no. CCDC-136800. Copies of the data can be obtained free of charge on application to CCDC, 12 Union Road, Cambridge CB2 1EZ, UK (fax: (+44) 1223-336-033; e-mail: deposit@ccdc.cam.ac.uk).

[15] Analysis of the holes was performed with the PLATON program (A. L. Spek, PLATON, Utrecht University, **1999**). The representation of the surfaces of the cavities was obtained with SURFNET; R. A. Laskowski, *J. Mol. Graph.* **1995**, *13*, 323.

[16] Refinement of the unit cell parameters on the XRPD spectra at room temperature gave $a = 28.06$, $b = 17.68$, $c = 30.88$ Å, $\beta = 109.1^\circ$, and $V = 14476$ Å^3. The increased dimensions with respect to the single crystal data at 223 K can be attributed mainly to thermal expansion.

[17] Differential scanning calorimetry (DSC) analysis shows a broad exothermic peak (40–120 °C) with its maximum at 90 °C and a minor complex event at 160–190 °C..

[18] Exchange with other polar solvents (methanol, acetonitrile) has also been successful. Samples of **1** dried at 100 °C and left in the presence of vapors of the polar solvent gave rather different XRPD spectra but after desolvation and rehydration with water vapors again show the original spectrum.

[19] This contrasts with that observed in the (reversible) desolvation of a recently reported hydrogen-bonded framework compound of remarkable flexibility that transforms into a second (dehydrated) monocrystalline form:C. J. Kepert, D. Hesek, P. D. Beer, M. J. Rosseinsky, *Angew. Chem.* **1998**, *111*, 3335; *Angew. Chem. Int. Ed.* **1998**, *37*, 3158.

[20] The nonrigidity of catenated networks with flexible ligands is confirmed by a 3D array of interpenetrated ladders that expands by enclathration of *p*-dibromobenzene while maintaining the same topology: M. Fujita, O. Sasaki, K.-Y. Watanabe, K. Ogura, K. Yamaguki, *New J. Chem.* **1998**, 189.

Asymmetric Synthesis of an Organic Compound with High Enantiomeric Excess Induced by Inorganic Ionic Sodium Chlorate**

Itaru Sato, Kousuke Kadowaki, and Kenso Soai*

Recent progress in asymmetric synthesis has been made by the developments of both organic asymmetric catalysts and stoichiometric organic chiral auxiliaries.[1] The origin of significant enantiomeric enrichments in organic compounds such as L-amino acids on the earth has been an intriguing puzzle.[2] One of the proposed mechanisms for the enantiomeric enrichments of organic compounds is through asymmetric synthesis and/or subsequent asymmetric adsorption[3] on the surface of inorganic enantiomorphic crystals. We recently reported an enantioselective synthesis of an organic compound promoted by chiral quartz,[4] which is an enantiomorphic inorganic molecule with covalent bonds between the silicon and oxygen atoms.

On the other hand, sodium chlorate ($NaClO_3$) is an enantiomorphic inorganic ionic crystal.[5] Kondepudi et al. reported that almost all of the $NaClO_3$ crystals precipitated from a stirred particular solution have the same chirality.[6, 7] However, the relevance of the chirality of $NaClO_3$ to that of an organic compound was not established. An earlier report[8] on the enantioselective adsorption of racemic compounds by $NaClO_3$ was disproved by the later examination of Gillard and da Luz de Jesus.[9] Thus, the question has remained as to whether significantly enantiomerically enriched organic compound can be formed using chiral $NaClO_3$, an inorganic ionic crystal.

Herein we report an unprecedented highly enantioselective synthesis of an organic compound which is induced by *d*- or *l*-$NaClO_3$ crystals. The enantioselective addition of diisopropylzinc (*i*Pr_2Zn) to 2-(*tert*-butylethynyl)pyrimidine-5-carbaldehyde (**1**) in the presence of *d*- or *l*-$NaClO_3$ powder gave pyrimidylalkanol **2** with high *ee* values (96–98% *ee*) in high yields (90–99%; Scheme 1, Table 1).

The (*S*)-pyrimidylalkanol (*S*)-**2** was obtained with 98% *ee* in 93% yield when *i*Pr_2Zn was added to the mixture of *d*-$NaClO_3$ and aldehyde **1** (Entry 1). The reaction is reproducible (Entries 2 and 3). On the other hand, reactions between aldehyde **1** and *i*Pr_2Zn in the presence of *l*-$NaClO_3$, instead of *d*-$NaClO_3$, always gave (*R*)-**2** with 98% *ee* in yields of 91–98% (Entries 4–6). When the reactions were run sequentially in the presence of *d*-, *l*-, *d*-, and *l*-$NaClO_3$, using exactly the same reaction equipments, (*S*)-, (*R*)-, (*S*)-, and (*R*)-**2** with

[*] Prof. Dr. K. Soai, Dr. I. Sato, K. Kadowaki
Department of Applied Chemistry
Faculty of Science, Science University of Tokyo
Kagurazaka, Shinjuku-ku, Tokyo 162-8601 (Japan)
Fax: (+81) 3-3235-2214
E-mail: ksoai@ch.kagu.sut.ac.jp

[**] This work was supported by a Grant-in-Aid for Scientific Research from the Ministry of Education, Science, Sports, and Culture. We thank Mr. Koji Ohtake for experimental work in the early stage, Prof. Naoyuki Koide and Dr. Takashi Mihara from the Department of Chemistry of our university for a microscope measurement of the size of the powdered $NaClO_3$.

  0044-8249/00/11208-1570 $ 17.50+.50/0